Quasi normal mode of Kerr black hole and Kerr Ads black hole at extremal limit

M.Sc. Thesis

By

Arijit Paul

(Roll Number: 2303151007)

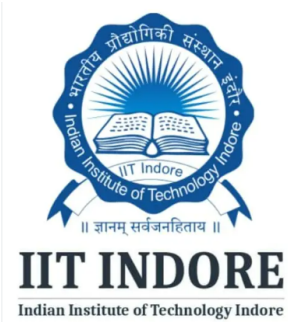

Under the guidance of

Prof.Manavendra Mahato

Department of Physics

Indian Institute of Technology Indore

May 2025

Quasi normal mode of Kerr black hole and Kerr Ads black hole at extremal limit

A THESIS

Submitted in partial fulfillment of the
requirements for the award of the degree

Master of Science

By

Arijit Paul

(Roll Number: 2303151007)

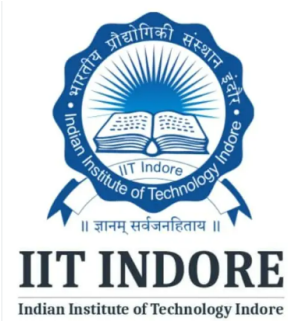

Department of Physics

Indian Institute of Technology Indore

May 2025

INDIAN INSTITUTE OF TECHNOLOGY INDORE

CANDIDATE'S DECLARATION

I hereby certify that the work which is being presented in the thesis entitled ***Quasi normal mode of Kerr black hole and Kerr Ads black hole at extremal limit*** in the partial fulfillment of the requirements for the award of the degree of **MASTER OF SCIENCE** and submitted in the **DEPARTMENT OF PHYSICS**, Indian Institute of Technology Indore, is an authentic record of my own work carried out during the time period from *August 2023* to *May 2025* under the supervision of *Prof.Manavendra Mahato , Professor, Department of Physics, IIT Indore*.

The matter is presented in this thesis, which has not been submitted by me for the award of any other degree of this or any other institute.

Arijit Paul (19.05.25)

Signature of the student with date

(Arijit Paul)

This is to certify that the above statement made by the candidate is correct to the best of my/our knowledge.

19/5/2025

Signature of the Supervisor of

M.Sc. thesis #1 (with date)

(Prof. Manavendra Mahato)

Arijit Paul has successfully given his M.Sc. Oral Examination held on **May 2025**.

19/5/2025

Signature(s) of Supervisor(s) of MSc thesis

Date:

Dipankar Das

Convener, DPGC

Date: 23-05-25

Signature of PSPC Member #1

Date:

Signature of PSPC Member #2

Date:

1 Abstract

This report is based on the quasi normal mode of Kerr black hole for massless spin-s field perturbation and also focused on the quasi normal mode of Kerr Ads black hole at extremal limit for scalar perturbation.

At first we discuss Kerr black hole's properties and the role of Killing -Yano tensor in generating conserved quantities which simplify the study of geodesic motion, wave propagation etc .We also analyze geometric structure of Kerr black hole at extremal limit and at near horizon limit . Furthermore, we establish a correspondence between high-frequency QNMs (eikonal regime) and unstable photon orbits, demonstrating how the real part of QNM frequencies relates to orbital energy and angular momentum, while the imaginary part encodes instability via Lyapunov exponents.

Due to disturbance of black hole by some external perturbation, the quasi normal mode tells about the oscillation.They are defined by complex frequency which give information about properties of black hole .The Teukolsky equation describes the perturbation of black hole and for the Kerr black hole it is divided into two parts, one is radial and another one is angular in Boyer-Lindquist coordinates.Solution for both parts are made by series solution and the coefficients follow some recurrence relation.By using it, the QNF(Quasi normal frequency) are derived numerically for different field spin . This analysis offers a comprehensive framework to study black hole perturbation and also the results are compared with Leaver's paper .We here also try to find quasi normal frequencies for others different spin field perturbation like s=-1 for electromagnetic field and s=0 for outgoing scalar field .

After that,I try to find the quasi-normal modes of a Kerr-AdS black hole in the extremal limit under scalar perturbations, and demonstrate that it remains linearly stable in this extremal case.

Contents

2 Introduction

Quasi-normal frequencies (QNF) are like the ”ringing” of a black hole after it’s disturbed, such as when a gravitational wave passes through it. These frequencies have two parts: one describes the oscillation (real part) and the other describes how quickly the oscillations fade (imaginary part). They help us to understand how a black hole ”responds” to disturbances. At the time of the study on how gravitational waves scatter off black holes, in 1970 Vishveshwara first discovered the complex resonant frequencies corresponding to them.

What Happens When a Black Hole Is Disturbed?

When a gravitational wave or matter hits a black hole, it disturbs the spacetime around it, causing the black hole to ”vibrate.” This vibration is the black hole’s quasinormal modes (QNM), which are the natural frequencies it oscillates after being disturbed. For Kerr black holes, which are rotating, the oscillations are more complex due to their angular momentum.

Why Do Quasi-Normal Frequencies Matter?

These frequencies are crucial for understanding black holes, especially in gravitational wave astronomy. When two black holes merge, the final black hole ”rings” during a phase called ”ringdown,” and the frequencies of this ringing tell us about its mass, spin, and other properties.

Key Features of Quasi-Normal Frequencies in Kerr Black Holes

Infinite Frequency: A rotating Kerr black hole has infinite quasi-normal frequencies. Higher Modes: As the black hole spins faster, the frequencies become more evenly spaced, and high-order modes merge into a single, undamped mode.

Importance for Gravitational Wave Astronomy

Quasi-normal frequencies are key to understanding gravitational waves from black hole mergers. By analyzing the ”ringdown” phase (The ringdown phase in a Kerr black hole is the final stage after an event like a black hole merger, where the disturbed black hole settles into a stable state. This phase is dominated by quasi-normal modes (QNMs)—damped oscillations of spacetime caused by the black hole’s return to equilibrium), scientists can determine the mass and spin of the newly formed black hole, offering insights into its properties.

2.1 Physical Interpretation of Quasi-Normal Modes (QNMs)

Quasi-normal modes (QNMs) can be understood in physical terms, particularly in relation to **decay processes** in a black hole's dynamics. Here's how they relate to decay and their physical meaning:

Oscillatory Behavior (Real Part of the Frequency)

The **real part** of a quasi-normal mode frequency represents the natural oscillation frequency of spacetime around the black hole. This is analogous to the "tone" of the black hole's vibration, similar to the ringing of a bell after it is struck.

Damping or Decay (Imaginary Part of the Frequency)

The **imaginary part** of the frequency describes the rate at which the oscillations decay over time. This decay occurs as energy is radiated away in the form of gravitational waves, causing the vibrations to fade and the black hole to return to a steady state.

Physical Insight:

The decay reflects the stability of the black hole. The fact that the oscillations decay (rather than grow) ensures that the black hole stabilizes after being disturbed.

Why Do These Oscillations Decay?

The decay arises because the vibrations are not confined to the black hole; instead, energy escapes as **gravitational waves**. These waves carry the disturbance's energy outward, calming the black hole.

Analogy: Think of a pebble dropped into a pond. The ripples spread outward and lose energy as they propagate, eventually leaving the pond's surface calm. Similarly, gravitational waves carry the black hole's vibrational energy outward, causing the QNM amplitudes to decay.

Role of Decay in the Ringdown Phase

During the **ringdown phase** following a black hole merger, the newly formed black hole vibrates in its quasi-normal modes. The frequencies and decay rates observed in gravitational waves provide critical information about:

- The speed with which the black hole settles into a stable state is measured.
- The black hole's mass and spin, which influence the QNM frequencies and decay timescales.

Mathematical Connection to Decay

Mathematically, QNMs are solutions to perturbation equations with complex frequencies:

$$\omega = \mathrm{Re}(\omega) + i\mathrm{Im}(\omega),$$

where:

- $\mathrm{Re}(\omega)$: Describes the oscillatory behavior (how fast spacetime oscillates).
- $\mathrm{Im}(\omega)$: Describes the decay rate (how quickly the oscillations fade).

The decay time (τ) is inversely proportional to $|\mathrm{Im}(\omega)|$:

$$\tau \propto \frac{1}{|\mathrm{Im}(\omega)|}.$$

A larger $|\mathrm{Im}(\omega)|$ implies faster damping.

Broader Physical Meaning

QNMs provide a way to understand **how spacetime itself responds** to disturbances, revealing that:

- Spacetime behaves like a damped resonator.
- The decay rate measures how efficiently gravitational waves carry energy away.

In essence, QNMs describe the "ringing" of spacetime and its "calming down," offering insights into the dynamic and dissipative nature of black holes.

3 Properties of Kerr black hole

In Boyer-Lindquist coordinates, the Kerr metric is [1]

$$ds^2 = -\frac{\Delta}{\rho^2}dt^2 - a\sin^2\theta d\phi dt + \frac{\rho^2}{\Delta}dr^2 + \rho^2 d\theta^2 + \sin^2\theta\left(\frac{(r^2+a^2)}{\rho^2}d\phi^2\right), \qquad (1)$$

where

$$\Delta = r^2 - 2Mr + a^2, \quad \rho^2 = r^2 + a^2 \cos^2 \theta. \tag{2}$$

Here, $a = \frac{J}{M}$ t. The inner (r_-) and outer (r_+) horizons are found by the roots of the equation $\Delta = 0$:

$$r_\pm = M \pm \sqrt{M^2 - a^2}. \tag{3}$$

In the case for the Schwarzchild black hole where $a = 0$, we find $r_+ = 2M$. In the extremal case where $a = M = \sqrt{J}$, the inner and outer horizons coincide with each other at $r_+ = M$. If $J > M^2$, the expressions for the naked ring singularity at $r = 0$, which violates the cosmic censorship conjecture tells us that the angular momentum must satisfy $J \leq M^2$.

This limitation can also be understood through the angular velocity of the horizon. [1]

$$\Omega_H = \frac{a}{2Mr_+}. \tag{4}$$

.

Bekenstein and Hawking found that black holes possess a temperature and an entropy given by [1]:

$$T_H = \frac{r_+ - M}{4\pi M r_+}, \quad S = 2\pi M r_+. \tag{5}$$

At $a = M$, the temperature T_H becomes zero, showing that these extremal rotating black holes represent a kind of ground state. Generally they are more easier than analyzing excited states [1].

3.1 Killing-Yano Tensor

A **Killing-Yano tensor** is an important concept in differential geometry and theoretical physics, particularly in the study of spacetimes with specific symmetries, such as the Kerr geometry in general relativity. Here's a summary of its key properties and significance:

3.1.1 Definition

A Killing-Yano tensor $f_{\mu\nu}$ is an antisymmetric tensor that satisfies the following conditions:

1. **Antisymmetry**:

$$f_{\mu\nu} = -f_{\nu\mu}. \tag{6}$$

2. **Covariant derivative :**

$$\nabla_{(\rho} f_{\mu)\nu} = 0, \tag{7}$$

which means that the covariant derivative of $f_{\mu\nu}$ is symmetric in the indices ρ and μ.

3.1.2 Properties

- **Similar to Killing vectors**: While Killing vectors satisfy the equation [2]

$$\nabla_\mu K_\nu + \nabla_\nu K_\mu = 0, \tag{8}$$

Killing-Yano tensors are more general due to their antisymmetry.

- **Geodesic Motion**: To analyze particles of motion, we need conserved quantities that can be derived by Killing Yano tensor. **Killing tensor**:for a KYT $f_{\lambda\nu}$,we can make symmetric tensor [3]

$$K_{\mu\nu} = f^\lambda_\mu f_{\lambda\nu}, \quad \nabla_{(\mu} K_{\nu\rho)} = 0 \tag{9}$$

which is a Killing tensor [3]. Let a Lagrangian $L : T(M) \to R$ have a continuous symmetry under an infinitesimal transformation which is given by $\delta x^\mu \equiv \varepsilon R^\mu(x,p)$ where R^μ is a rank-1 Killing tensor . Then there will exist a corresponding conserved charge which is given by [3]

$$J = \int \mathrm{d}x_\mu \frac{\partial L}{\partial x^\mu}, \tag{10}$$

when x^μ obeys the equations of motion.

Proof. A symmetry transformation must give us $\delta L \equiv 0$. $\hat{\delta} x^\mu$ and $\hat{\delta}\dot{x}^\mu$ using this expression , and we can get:

$$0 = \delta L = L\left(x + \hat{\delta} x^\mu, \dot{x} + \hat{\delta}\dot{x}^\mu\right) - L(x,\dot{x}) = L\left(x + \varepsilon R^\mu, \dot{x} + \varepsilon \dot{R}_\mu\right) - L(x,\dot{x}). \tag{11}$$

This can be expanded as:

$$= L(x,\dot{x}) + \frac{\partial L(x,\dot{x})}{\partial x^\mu}\varepsilon R^\mu + \frac{\partial L(x,\dot{x})}{\partial \dot{x}^\mu}\varepsilon \dot{R}^\mu - L(x,\dot{x}) = \frac{\partial L(x,\dot{x})}{\partial x^\mu} R^\mu + \frac{\partial L(x,\dot{x})}{\partial \dot{x}^\mu}\dot{R}^\mu. \tag{12}$$

Applying the equations of motion $\frac{\partial L(x,\dot{x})}{\partial x^\mu} = \frac{d}{d\tau}\frac{\partial L(x,\dot{x})}{\partial \dot{x}^\mu}$,putting in equation 12,we will get

$$0 = \frac{\partial L(x,\dot{x})}{\partial x^\mu} R^\mu + \frac{\partial L(x,\dot{x})}{\partial \dot{x}^\mu}\dot{R}^\mu = \frac{d}{d\tau}\left(\frac{\partial L(x,\dot{x})}{\partial \dot{x}^\mu} R^\mu\right). \tag{13}$$

Thus we have that

$$J \equiv \frac{\partial L(x,\dot{x})}{\partial \dot{x}^\mu} R^\mu, \tag{14}$$

is conserved along the equations of motion, as we wanted to show.

Lagrangian has the geodesic equation as EOM is the single-particle Lagrangian

$$L(x,\dot{x}) = \frac{1}{2} g_{\mu\nu}\dot{x}^\mu \dot{x}^\nu, \tag{15}$$

which is basically a “free particle” Lagrangian, with corresponding Hamiltonian

$$H(x,p) = \frac{1}{2} g^{\mu\nu} p_\mu p_\nu.$$

In this case, equation tells us that the conserved quantity is

$$J = \frac{\partial L(x,\dot{x})}{\partial \dot{x}^\mu} R^\mu = p_\mu R^\mu. \tag{16}$$

3.1.3 Significance

- **Conserved Quantities**: The existence of Killing-Yano tensors tells us about additional conserved quantities, which can be very useful in studies of geodesic equations of any particle.

- **Geometric Structures**: They contribute to the understanding of the geometric structures of the manifold and can help in deriving important results in both mathematics and theoretical physics.

Killing-Yano tensors thus represent a fascinating aspect of the interplay between symmetry and geometry in the study of curved spacetimes.

In this discussion, we explore the near-horizon region of an extremal Kerr black hole, where the complexities of the full Kerr geometry become significantly simplified. This simplification often occurs in physics when examining systems in limiting cases, such as low-energy conditions in condensed matter physics, where detailed atomic behavior can be overlooked.

3.2 Extremal Limit

For an extremal Kerr black hole, characterized by $a = M$, various formulas become much simpler [4]:

$$\begin{aligned} r_{\pm} &= a = M, \\ S &= 2\pi M^2 = 2\pi J, \\ T_H &= 0, \\ \Omega_H &= \frac{1}{2M}. \end{aligned}$$

The metric for the extremal Kerr geometry reduces to [4]:

$$ds^2 = -\frac{\Delta}{\rho^2}\left(dt - a\sin^2\theta d\phi\right)^2 + \frac{\rho^2}{\Delta}dr^2 + \sin^2\theta\rho^2\left((\hat{r}^2+a^2)d\phi - adt\right)^2 + \rho^2 d\theta^2, \qquad (17)$$

where

$$\Delta = (\hat{r}-a)^2, \quad \rho^2 = \hat{r}^2 + a^2\cos^2\theta. \qquad (18)$$

3.3 Near-Horizon Limit

To study the near-horizon region, we introduce a scaling parameter $\lambda \to 0$ while focusing on the vicinity of $r = M$. We redefine the coordinates as follows [4]:

$$\begin{aligned} r &= \hat{r} - \frac{M}{\lambda M} & dr &= \hat{d}r \\ t &= \frac{\lambda\hat{t}}{2M} & dt &= \frac{\lambda}{2M}\hat{d}t \\ \phi &= \hat{\phi} - \frac{\hat{t}}{2M} & d\phi &= \hat{d}\phi - \frac{1}{2M}\hat{d}t \end{aligned}$$

after puttings new coordintaes $\rho^2 = \hat{r}^2 - \frac{2}{\lambda}\hat{r} + \frac{1}{\lambda} + a^2 cos^2\theta$ and $\Delta = \hat{r}^2 - \frac{2}{\lambda}\hat{r} + \frac{1}{\lambda} - 2\hat{r}a + 2\frac{a}{\lambda} + a^2$

In this limit, we can derive a smoother geometry represented by [1]:

$$ds^2 = 2\Omega^2 J \left(\frac{dr^2}{r^2} + d\theta^2 - r^2 dt^2 + \Lambda^2 (d\phi + r dt)^2 \right), \tag{19}$$

where the functions Ω and Λ are given by:

$$\Omega^2 = \frac{1+\cos^2\theta}{2}, \quad \Lambda = \frac{2\sin\theta}{1+\cos^2\theta}. \tag{20}$$

This expression is known as the near-horizon extremal Kerr geometry (NHEK). Notably, the black hole's angular momentum J factors out in front of the metric, indicating that it is a solution to the Einstein equations, albeit not asymptotically flat [4].

3.4 Geodesic Motion in Kerr Spacetime

In the study of black holes, particularly the *Kerr black hole* (which rotates), particles and light follow paths called *causal geodesics*. These paths are influenced by the black hole's strong gravity. The tangent vector $\dot{x}^\mu = \frac{dx^\mu}{d\lambda}$ describes how the particle moves along these paths, with λ being a parameter (like time for massive particles or an affine parameter for light). The condition $g_{\mu\nu}\dot{x}^\mu\dot{x}^\nu = 0$ (for light) or -1 (for massive particles) ensures the particle stays on its geodesic.

Due to the Kerr black hole's symmetries—*stationarity* (unchanging in time) and *axisymmetry* (symmetry around its rotation axis)—two quantities are conserved along the geodesic:

1. **Energy** (e): A measure of the particle's energy, derived from the time symmetry. For a particle with rest mass μ, it's given by

$$e = -\mu\, g_{\mu\nu}\dot{x}^\nu (\partial_t)^\mu. \tag{21}$$

2. **Angular Momentum** (j): A measure of the particle's rotational motion around the black hole, derived from the axisymmetry. It's expressed as

$$j = \mu\, g_{\mu\nu}\dot{x}^\nu (\partial_\phi)^\mu. \tag{22}$$

In 1968, physicist **Brandon Carter** discovered a third conserved quantity, now called the *Carter constant* (Q), which is more subtle and arises from a hidden symmetry of the Kerr spacetime. This constant is *quadratic* in the particle's momentum (unlike e and j, which are

linear). In Boyer-Lindquist coordinates (a common coordinate system for Kerr black holes), it takes the form:

$$Q = \mu^2 \dot{\theta}^2 + \cos^2\theta \left[a^2(\mu^2 - e^2) + \left(\frac{j}{\sin\theta} \right)^2 \right], \tag{23}$$

where:

- $\dot{\theta}$ is the derivative of the polar angle θ (how the particle moves in the "up-down" direction relative to the black hole's equator).
- a is the black hole's spin parameter.
- The term $\cos^2\theta$ shows how the constant depends on the particle's latitude.

A related quantity, $K = Q + (j - ae)^2$, is often used because it's always non-negative, making it more convenient for analysis. The existence of Q (or K) is crucial because it allows geodesic motion in Kerr spacetime to be *integrable*—meaning the equations of motion can be solved systematically, much like how conservation laws simplify problems in Newtonian mechanics.

3.4.1 Why is this important?

The Carter constant helps physicists predict the exact paths of particles and light around rotating black holes, which is essential for understanding phenomena like accretion disks, gravitational lensing, and even the signatures of black holes in astrophysical observations. Without it, the motion would appear chaotic, but Carter's discovery revealed an underlying order in the Kerr spacetime's structure.

3.4.2 Black Hole Vibrations and Light Paths: A Deep Connection

When studying how black holes vibrate (through their "quasi-normal modes") and how light behaves near them, physicists have discovered a beautiful mathematical connection between waves and particle paths. This relationship becomes especially clear when we examine high-frequency waves (where the angular momentum number l is very large) - what we call the *eikonal regime* or *geometric optics approximation*.

3.4.3 From Wave Equations to Light Paths

In this high-frequency limit, the complicated Teukolsky equations (which describe perturbations of rotating black holes) simplify to a form that resembles quantum mechanical problems:

$$\varepsilon f''(z) + U(z) f(z) = 0 \tag{24}$$

where ε is very small. We can solve this using WKB approximation methods (similar to those in quantum mechanics), writing the solution as:

$$f(z) \sim \exp\left(\frac{S_0}{\varepsilon} + S_1 + \varepsilon S_2 + \cdots\right) \tag{25}$$

This mathematical approach reveals something remarkable: every vibrational mode of the black hole corresponds exactly to a specific path that light would take around the black hole!

3.4.4 The Wave-Particle Dictionary

Just like in quantum mechanics where particles can behave as waves, here we find a perfect correspondence:

- **Frequency is energy**: The real part of the wave frequency $\mathrm{Re}(\omega_{lmN})$ equals the energy e of the corresponding light path.
- **Azimuthal number is angular momentum**: The quantum number m matches the z-component of the light path's angular momentum j. This quantization creates standing waves in the ϕ (azimuthal) direction.
- **Separation constant relates to Carter's constant**: The real part of $\mathscr{E}_{lm\omega}$ connects to both Carter's constant Q and the squared angular momentum j^2. This leads to quantization in the θ (polar) direction too, creating standing waves.
- **Decay Rate reveals instability**: The imaginary part $\mathrm{Im}(\omega_{lmN})$ equals a Lyapunov exponent γ_L, which measures how unstable the light path is - showing how quickly nearby paths diverge.

3.4.5 Why This Matters: Black Hole Spectroscopy

This correspondence is incredibly powerful because:

- It lets us understand black hole vibrations by studying simpler light paths
- Provides a way to ”fingerprint” black holes through their vibration patterns
- Helps connect quantum effects with general relativity
- May lead to new ways to detect black holes through their gravitational waves

3.5 Different Perturbations

3.5.1 1. Gravitational Perturbations (Spin-2 Field)

- Governed by the **Teukolsky equation** for spin $s = -2$.
- The QNMs are crucial for modeling **ringdown signals** in gravitational-wave astronomy (e.g., from black hole mergers).
- For slowly rotating black holes ($a \ll M$), the frequencies can be approximated analytically, but for high spins, numerical methods (e.g., Leaver's continued fraction method or spectral methods) are required.
- For high spins ($a \approx M$), the **superradiant modes** (where $\mathrm{Im}(\omega) > 0$) can appear, leading to instabilities.

3.5.2 2. Electromagnetic Perturbations (Spin-1 Field)

- Described by the Teukolsky equation for $s = -1$.
- The QNMs are less damped than gravitational ones.
- For Kerr black holes, the modes split due to rotation (**prograde vs. retrograde modes**).

3.5.3 3. Massless Scalar Field Perturbations (Spin-0 Field)

- Obey the Klein-Gordon equation in Kerr spacetime (Teukolsky equation for $s = 0$).
- Massless scalar fields are often used to study gauge-invariant cosmological perturbations.
- For rotating black holes, **superradiant amplification** can occur if $\mathrm{Re}(\omega) < m\Omega_H$, where Ω_H is the horizon angular velocity.

3.6 Methods to find Kerr Black Hole Quasinormal Modes (QNMs)

1. **Time Domain Simulation**

   This approach directly simulates how perturbations evolve over time. It's especially useful for modeling the "ringdown" phase of black hole mergers—something LIGO relies on for detecting gravitational waves.

2. **Continued Fraction Method (Leaver's Method)**

   A mathematically powerful technique that solves complex equations using infinite fractions. It's known for delivering the most accurate results when studying Kerr black holes.

3. **WKB Approximation**

   Think of this like treating black hole vibrations as quantum waves tunneling through a barrier. It's quick and intuitive but loses accuracy when dealing with lower-frequency (low-overtone) modes.

4. **Monodromy Method**

   A deep, mathematically elegant technique that uses complex analysis to uncover asymptotic QNMs. It's not the easiest to grasp, but it offers fascinating insights into the black hole's structure.

5. **Shooting Method**

   This method "shoots" solutions from both the black hole's horizon and from infinity, adjusting until they match. It's straightforward but becomes unstable for black holes spinning rapidly.

6. **Green's Function Approach**

   A more theoretical route that views QNMs as poles in the black hole's scattering response. Rich in physics but often computationally intensive.

4 Quasi-normal modes for Rotating Black Holes

In 1972, Teukolsky gave a partial differential equation in Boyer-Lindquist coordinates t,r,θandϕ and also introduced the field quantities ψ which were separated into two parts, one radial and the other an angular part. So using this field quantity ψ we can get two partial differential equations for both the radial and the angular part. [7].

$$\psi(t,r,\theta,\phi) = \frac{1}{2\pi}\int e^{-i\omega t}\sum_{l=|s|}^{\infty}\sum_{m=-l}^{l} e^{im\phi}S_{lm}(u)R_{lm}(r)d\omega. \tag{26}$$

where $u = \cos\theta$ and the partial differential equation for both S_lm and R_lm are [5]

$$(1-u^2)\frac{d}{du}\left((1-u^2)\frac{dS_{lm}}{du}\right) + \left[a^2\omega^2u^2 - 2a\omega su + s + A_{lm} - (m+su)^2\right]S_{lm} = 0, \tag{27}$$

which is [7] Teukolsky's equation 8,

$$\Delta\frac{d}{dr}\left(\Delta\frac{dR_{lm}}{dr}\right) + (s+1)(2r-1)\frac{dR_{lm}}{dr} + V(r)R_{lm} = 0, \tag{28}$$

where the potential $V(r)$ is [3] Teukolsky's equation 7:

$$V(r) = \left[(r^2+a^2)\omega^2 - 2am\omega r + a^2m^2 + is(am(2r-1) - \omega(r^2-a^2))\right]\Delta^{-1} + \left[2is\omega r - a^2\omega^2 - A_{lm}\right], \tag{29}$$

where $\Delta = r^2 - r + a^2$. The rotation parameter a is the angular momentum per unit mass ($0 \le a \le \frac{1}{2}$), and the field spin parameter s = $0, -1$ and -2 for scalar, electromagnetic and grtavitationals, respectively. S_{lm} is finite at regular singular points for $u = +1$and -1 where the indices are $\frac{1}{2}(m+s)$ and$\frac{1}{2}(m-S)$, respectively.

4.1 Solution for angular part

The solution of equation 27 is written like [6]

$$S_{lm}(u) = e^{a\omega u}(1+u)^{\frac{1}{2}|m-s|}(1-u)^{\frac{1}{2}|m+s|}\sum_{n=0}^{\infty} a_n(1+u)^n \tag{30}$$

The recurrence relations for differential equation 27 are [5]

$$\alpha_\theta^0 a_1 + \beta_\theta^0 a_0 = 0 \tag{31}$$

$$\alpha_\theta^n a_{n+1} + \beta_\theta^n a_n + \gamma_\theta^n a_{n-1} = 0, \quad n = 1,2,\ldots \tag{32}$$

and the recurrence coefficients are [5]

$$\begin{aligned}
\alpha_\theta^n &= -2(n+1)(n+2k_1+1), \\
\beta_\theta^n &= n(n-1)+2n(k_1+k_2+1-2a\omega) \\
&\quad -[2a\omega(2k_1+s+1)-(k_1+k_2)(k_1+k_2+1)] \\
&\quad -\left[a^2\omega^2+s(s+1)+A_{lm}\right], \\
\gamma_\theta^n &= 2a\omega(n+k_1+k_2+s).
\end{aligned} \tag{33}$$

where $k_1 = \frac{1}{2}|m-s|$ and $k_2 = \frac{1}{2}|m+s|$

4.1.1 Continued fraction equation for angular part

For different values, a, m,s, and w, equation 31 and equation 32 will be satisfied.A_lm is the root of the below-continued fraction [5]

$$0 = \beta_0^\theta - \frac{\alpha_0^\theta\gamma_1^\theta}{\beta_1^\theta -}\frac{\alpha_1^\theta\gamma_2^\theta}{\beta_2^\theta -}\frac{\alpha_2^\theta\gamma_3^\theta}{\beta_3^\theta -}\cdots \tag{34}$$

4.2 Solution for radial part

To solve radial part, we follow same procedure just like how we solved for angular part.In R_{lm} differential equation(28);

$$\Delta = r^2 - r + a^2 \equiv (r - r_-)(r - r_+) \tag{35}$$

[5] where Δ has two roots r_- and r_+which are regular singular points .In the differential equation $b = \sqrt{1-4a^2}$ is used as rotation parameter where it ranges from 1 to 0 because a ranges from 0 to $\frac{1}{2}$ in Kerr limit.

We can write roots $r_\pm$ of Δ in the form of b [1] :

$$r_\pm = \frac{1}{2}(1 \pm b). \tag{36}$$

The event horizon corresponds to the larger root, $r = r_+$. The indices at $r = r_+$ are $i\sigma_+$ and $-s - i\sigma_+$, where:

$$\sigma_+ = \frac{\omega r_+ - am}{b}. \tag{37}$$

[5]

The second index, $-s - i\sigma_+$, represents in-going radiation.

4.2.1 Boundary Condition

The asymptotic solutions are [7]:

$$\lim_{r\to\infty} R_{lm}(r) \sim r^{-1-i\omega} e^{-i\omega r}, \tag{38}$$

and

$$\lim_{r\to\infty} R_{lm}(r) \sim r^{-1-2s+i\omega} e^{i\omega r}, \tag{39}$$

Equation(39) describes to outgoing radiation based on the sign convention established in equation (36) To solve radial differential equation,

$$R_{lm}(r) \xrightarrow{r\to r_+} (r - r_+)^{-s-i\sigma_+}, \tag{40}$$

[5] and

$$R_{lm}(r) \xrightarrow{r\to\infty} r^{-1-2s+i\omega} e^{i\omega r}. \tag{41}$$

[5]

These boundary conditions ensure that the solution represents purely ingoing waves at the event horizon $r = r_+$ and purely outgoing waves at spatial infinity [1]. since

$$R_{lm}(r) = e^{i\omega r}(r-r_-)^{-1-s+i\omega+i\sigma_+}(r-r_+)^{-s-i\sigma_+}\sum_{n=0}^{\infty} d_n \left(\frac{r-r_+}{r-r_-}\right)^n \tag{42}$$

4.2.2 Continued fraction for radial part

The recurrence relations are [5]

$$\alpha_r^0 d_1 + \beta_r^0 d_0 = 0, \tag{43}$$

$$\alpha_r^n d_{n+1} + \beta_r^n d_n + \gamma_r^n d_{n-1} = 0, \quad n = 1,2,\ldots \tag{44}$$

The recursion coefficients are given by [5]:

$$\alpha_r^n = n^2 + (c_0+1)n + c_0, \tag{45}$$

$$\beta_r^n = -2n^2 + (c_1+2)n + c_3, \tag{46}$$

$$\gamma_r^n = n^2 + (c_2-3)n + c_4 - c_2 + 2. \tag{47}$$

Inside the recursion coefficient , there are other coefficients c_n which are defined as follows [5]:

$$c_0 = 1 - s - i\omega - \frac{2i}{b}(\omega^2 - am), \tag{48}$$

$$c_1 = -4 + 2(2+b)i\omega + \frac{4i}{b}(\omega^2 - am), \tag{49}$$

$$c_2 = s + 3 - 3i\omega - \frac{2i}{b}(\omega^2 - am), \tag{50}$$

$$c_3 = \omega^2(4+2b-a^2) - 2am\omega - s - 1 - A_{lm} + (2+b)i\omega + \frac{4\omega+2i}{b}(\omega^2 - am), \tag{51}$$

$$c_4 = s + 1 - 2\omega^2 - (2s+3)i\omega - \frac{4\omega+2i}{b}(\omega^2 - am). \tag{52}$$

The continued fraction equation for the radial part [5]

$$0 = \beta_0^r - \frac{\alpha_0^r \gamma_1^r}{\beta_1^r -} \frac{\alpha_1^r \gamma_2^r}{\beta_2^r -} \frac{\alpha_2^r \gamma_3^r}{\beta_3^r -} \cdots \tag{53}$$

4.3 Result

It is a rotating black hole.Due to black hole's spin, the space time around this black hole is asymmetrically curved which is the reason behind the different types of fields like scalar,electromagnetic and gravitational field to behave differently and also by analyzing their result we can get to know how they interact with spacetime geometry as well as stability of these fields around the Kerr black hole.

After getting two continued fraction equations (34) and (53), we can find real and imaginary values of $A_{lm}$and ω. By using Python programming I try to find the values of A_{lm} and w **for the gravitational field** spin weight parameter (s)=-2.

Here I try to compare my data and Leaver's data.

Rotation Parameter (a)	A_{lm}		omega		Leaver's A_{lm}		Leaver's omega		Error	
	Real	Imaginary	Real	Imaginary	Real	Imaginary	Real	Imaginary	Real	Imaginary
For l = 2, M = 0										
0.0000	4.0000	0.00000	0.747343	-0.177925	4.0000	0.00000	0.747343	-0.177925	0.0%	0.0%
0.1000	3.9972	0.00139	0.750248	-0.177401	3.9972	0.00139	0.750248	-0.177401	0.0%	0.0%
0.2000	3.9886	0.00560	0.759363	-0.175653	3.9886	0.00560	0.759363	-0.175653	0.0%	0.0%
0.3000	3.9730	0.01262	0.776108	-0.171989	3.9730	0.01262	0.776108	-0.171989	0.0%	0.0%
0.4000	3.9480	0.02226	0.803835	-0.164313	3.9480	0.02226	0.803835	-0.164313	0.0%	0.0%
0.4500	3.9304	0.02763	0.824009	-0.156965	3.9304	0.02763	0.824009	-0.156965	0.0%	0.0%
0.4900	3.9127	0.03152	0.844509	-0.147065	3.9127	0.03152	0.844509	-0.147065	0.0%	0.0%
0.4999	3.9408	0.09265	0.805472	-0.1723	3.9077	0.03227	0.854023	-0.143646	5.2%	20%

Rotation Parameter (a)	A_{lm}		ω		Leaver's A_{lm}		Leaver'sω		Error	
	Real	Imaginary	Real	Imaginary	Real	Imaginary	Real	Imaginary	Real	Imaginary
For l = 2, M = 1										
0.0000	4.00000	-0.00000	0.747343	-0.177925	4.00000	-0.00000	0.747343	-0.177925	0.0%	0.0%
0.1000	3.89315	0.02520	0.776496	-0.176977	3.89315	0.02520	0.77650	-0.176977	0.0%	0.0%
0.2000	3.76757	0.05324	0.815958	-0.174514	3.76757	0.05324	0.815958	-0.174514	0.0%	0.0%
0.3000	3.61247	0.08347	0.871937	-0.169128	3.61247	0.08347	0.871937	-0.169128	0.0%	0.0%
0.4000	3.40228	0.11217	0.960461	-0.155910	3.40228	0.11217	0.960461	-0.155910	0.0%	0.0%
0.4500	3.29180	0.35643	1.031723	-0.14462	3.25345	0.11951	1.032583	-0.139609	2.0%	3.5%
0.4900	3.12479	0.29515	1.01447	-0.101783	3.07966	0.10216	1.012831	-0.103285	0.1%	1.4%

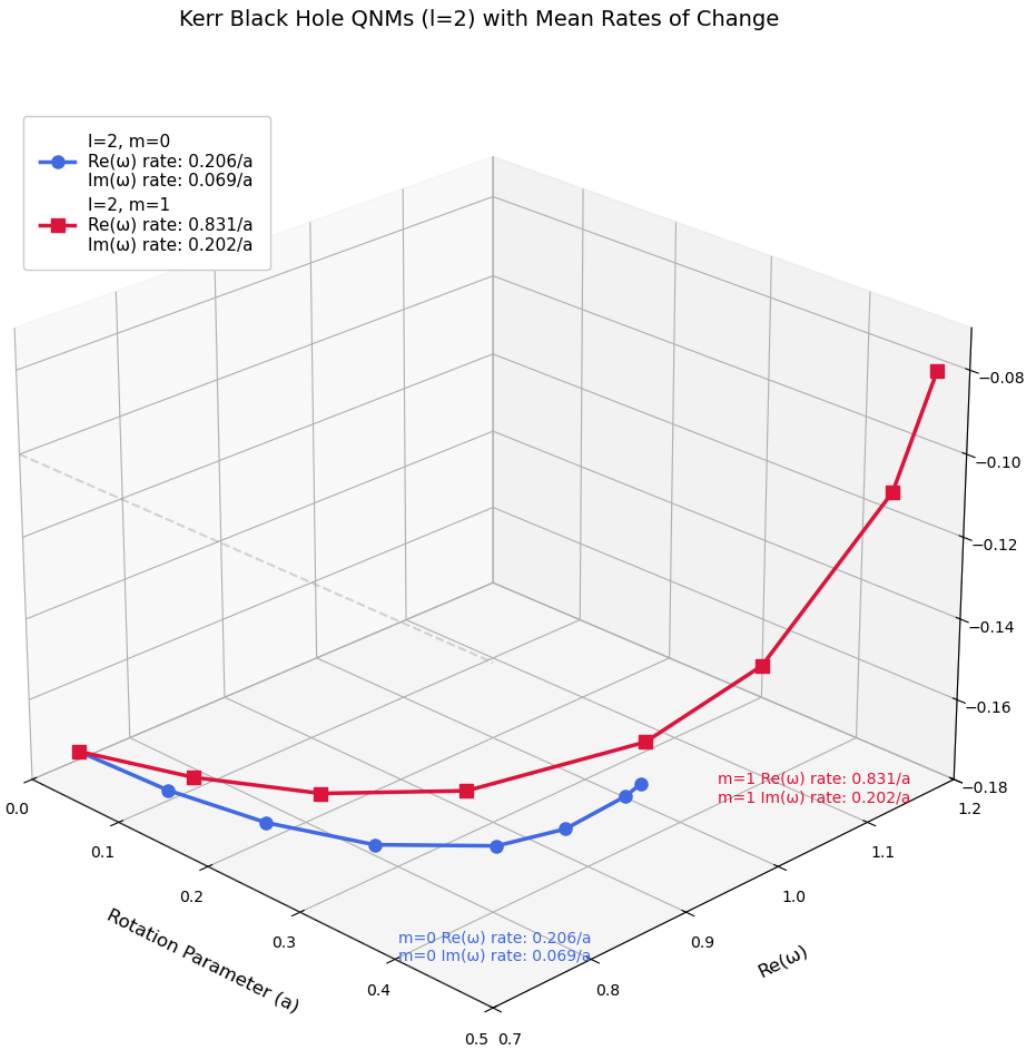

Figure 1: A 3D plot of the rotation parameter, real part of , and imaginary part of for gravitational field perturbations

4.3.1 For electromagnetic field

In the context of Kerr black hole , to know about how different type of field perturb black hole's spacetime and how it affects the oscillations , field spin weight parameter(s) plays a vital role in calculations.

here I also try to find quasi normal frequencies for electromagnetic field spin weight parameter(s)= -1 which is not shown in Leaver's paper

Rotation Parameter (a)	A_{lm}		omega	
	Real	Imaginary	Real	Imaginary
For l = 2, M = 0				
0.0000	2.00000	0.00000	0.496127	-0.184975
0.1000	5.99693	0.00132	0.917863	-0.189437
0.2000	5.98747	0.00528	0.926181	-0.187514
0.3000	5.97084	0.001180	0.941171	-0.183721
0.4000	5.94532	0.02058	0.960568	-0.176158
0.4500	5.92824	0.02538	0.981613	-0.169487
0.4900	5.93783	0.02538	0.981613	-0.169487

Rotation Parameter (a)	A_{lm}		omega	
	Real	Imaginary	Real	Imaginary
For l = 2, M = 1				
0.0000	2.00000	0.00000	0.496527	-0.184975
0.1000	5.96529	0.00719	0.947475	-0.189105
0.2000	5.92052	0.01764	0.989341	-0.186435
0.3000	5.86168	0.02798	1.045901	-0.180469
0.4000	5.78017	0.04239	1.129247	-0.166308
0.4500	5.72424	0.04648	1.191327	-0.150107
0.4900	5.66502	0.04321	1.262739	-0.119509

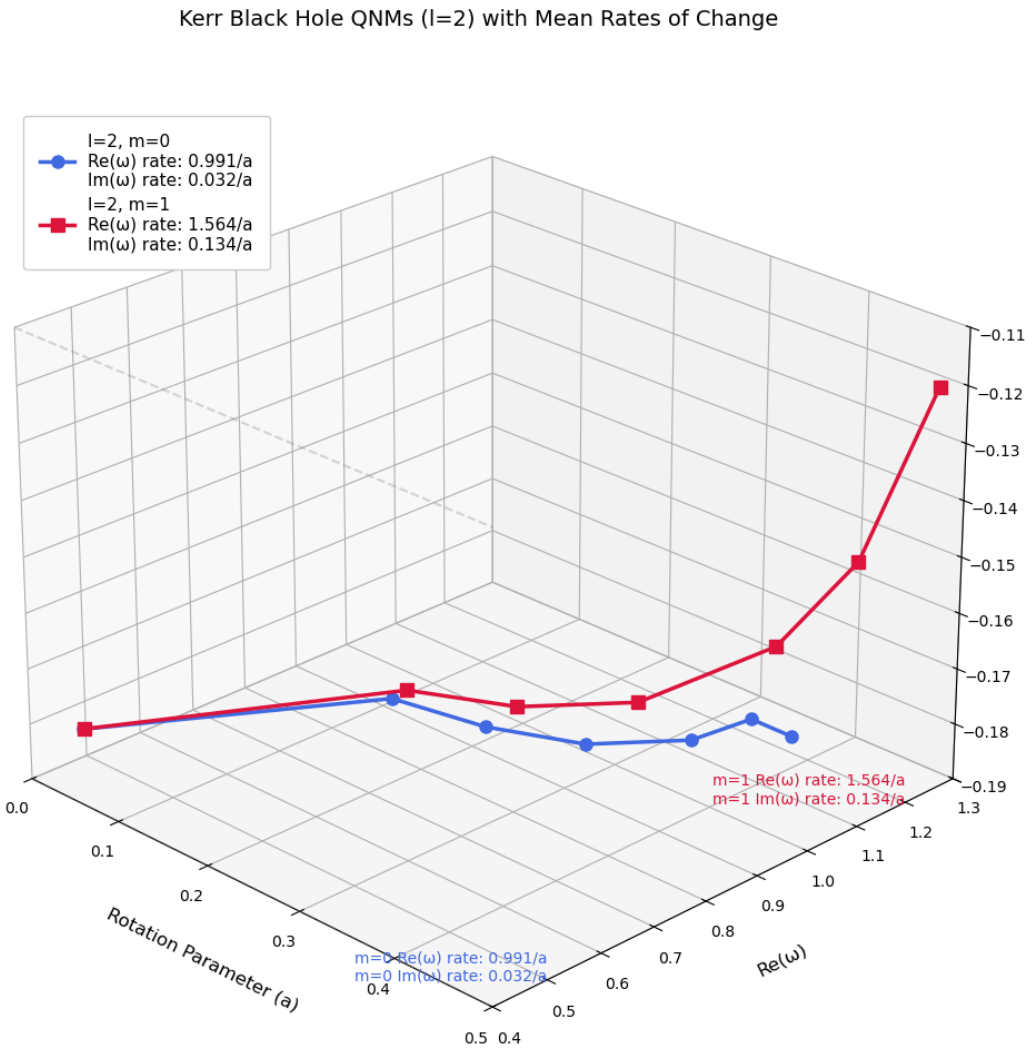

Figure 2: A 3D plot of the rotation parameter, real part of , and imaginary part of for electromagnetic field perturbations

4.3.2 For outgoing scalar field

Now ,for outgoing scalar field , we use spin weight field parameter (s)=0

Rotation Parameter (a)	A_{lm}		omega	
	Real	Imaginary	Real	Imaginary
For l = 2, M = 0				
0.0000	0.00000	0.00000	0.220910	-0.209791
0.1000	5.99527	0.00196	0.969828	-0.192911
0.2000	5.98075	0.00781	0.977720	-0.190930
0.3000	5.95533	0.01743	0.991877	-0.186962
0.4000	5.91671	0.03030	1.014245	-0.179339
0.4500	5.89112	0.03744	1.029558	-0.172813

Rotation Parameter (a)	A_{lm}		omega	
	Real	Imaginary	Real	Imaginary
For l = 2, M = 1				
0.0000	2.00000	0.00000	0.585872	-0.195320
0.1000	5.99586	0.00165	1.001109	-0.192822
0.2000	5.98192	0.00682	1.044284	-0.190295
0.3000	5.95447	0.01570	1.101598	-0.184382
0.4000	5.90568	0.02776	1.184035	-0.170251
0.4500	5.86749	0.03351	1.243657	-0.154350
0.4900	5.82458	0.03415	1.309412	-0.125797

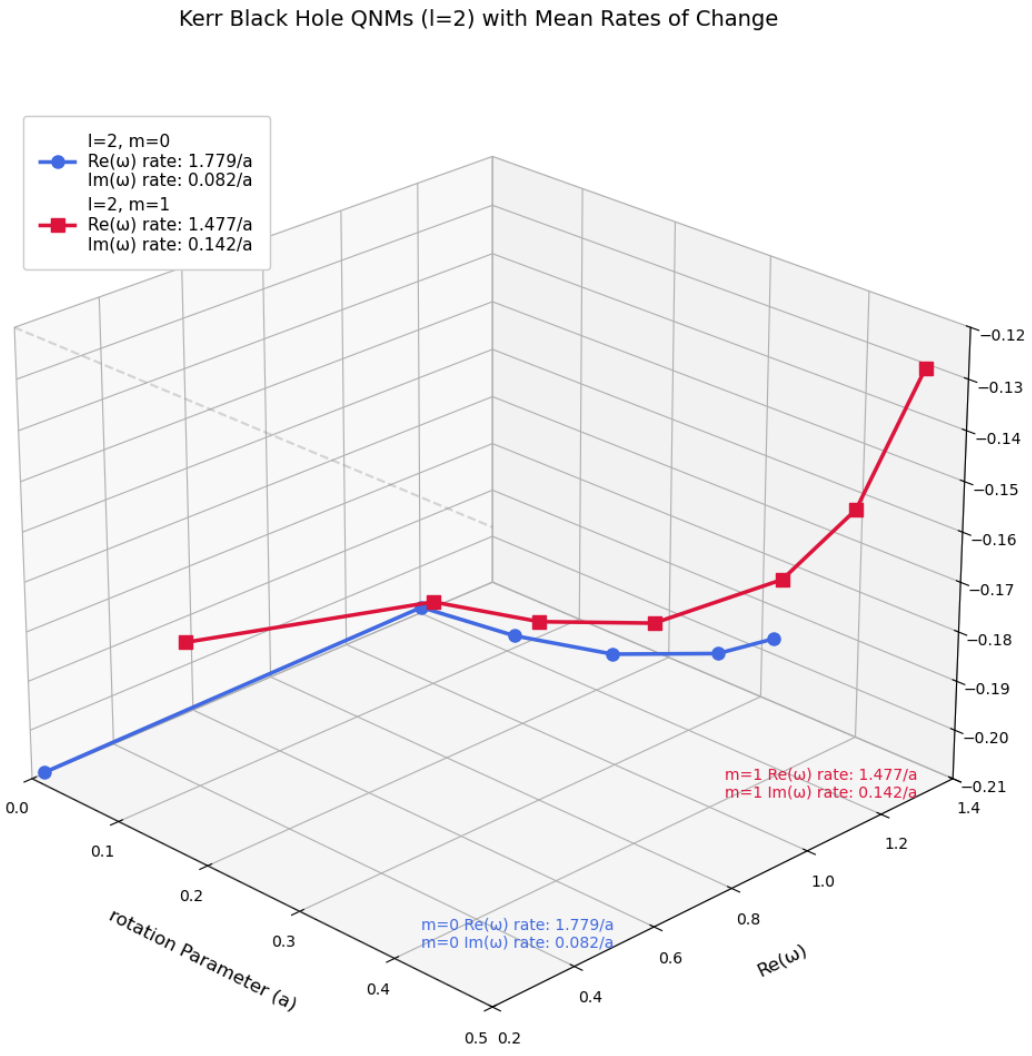

Figure 3: A 3D plot of the rotation parameter, real part of , and imaginary part of for outgoing scalar field perturbations

5 Conclusion

The constants l, m are two quantum numbers which basically give information about radial and angular wave functions. If we increase the azimuthal angle, quasi-normal frequencies (both oscillation frequency and decay rate) also increase.

Now if we look at a particular mode for different field perturbations:

Rotation Parameter (a)	Perturbation Type	ω	
		Real	Imaginary
For $l = 2, M = 0$			
0.3000	Gravitational field	0.776108	-0.171989
0.3000	Electromagnetic field	0.941171	-0.183721
0.3000	Outgoing scalar field	0.991877	-0.186962

As we know, $\mathrm{Re}(\omega)$ represents the frequency of oscillation and $\mathrm{Im}(\omega)$ represents the decay rate of oscillation. From the table we can observe that:

- $\mathrm{Re}(\omega)$ for outgoing scalar field perturbation is higher compared to other field perturbations
- $\mathrm{Im}(\omega)$ for outgoing scalar field perturbation is lower (less negative) than others

This result shows that for outgoing scalar field perturbations, a Kerr black hole takes more time to settle down to a stable state compared to other field perturbations (like electromagnetic or gravitational fields).

Furthermore, our numerical analysis confirms that $\mathrm{Im}\,\omega < 0$ for all modes, ensuring the absence of exponentially growing perturbations. This provides strong evidence for the *linear stability* of the Kerr black hole in Einstein gravity, as no unstable modes (with $\mathrm{Im}\,\omega > 0$) are present in the spectrum.

6 Kerr-AdS Black Hole

6.1 It's a Spinning Black Hole... But With a Twist

Think of the **Kerr black hole** (the classic spinning black hole), but instead of floating in empty space, it's inside a universe that curves inward (thanks to a **negative cosmological constant**,

$\Lambda < 0$).

This curvature means that far away from the black hole, space isn't flat—it's more like a gravitational well with walls.

6.2 The AdS Effect: A Cosmic Echo Chamber

In normal space, things fly away forever. But in **AdS space**, the curvature bends light and matter back, like a mirror.

This means the black hole's energy can bounce around, leading to wild effects like **superradiance** (where the black hole's spin amplifies waves, like a microphone feedback screech).

6.3 Two Horizons & a Warped Space Pool

Just like a regular Kerr black hole, it has:

- An **outer event horizon** (the point of no return)
- An **inner Cauchy horizon** (where physics gets weird)

But the AdS curvature changes their shapes and sizes, making the black hole's surroundings even more extreme.

7 Quasi normal mode of Kerr Ads Black hole at extremal limit for scalar perturbation

A Kerr–Anti-de Sitter (Kerr-AdS) black hole is a rotating black hole that exists in a negative-curvature spacetime (Anti-de Sitter space). It combines the features of a Kerr black hole (rotating with mass and angular momentum) with the geometry of AdS space, which has a negative cosmological constant. The line element for Kerr Ads black hole is [8]:

$$ds^2 = -\frac{\Delta_r}{\rho^2}\left(dt - \frac{a}{\Sigma}\sin^2\theta d\phi\right)^2 + \frac{\rho^2}{\Delta_r}dr^2 + \frac{\rho^2}{\Delta_\theta}d\theta^2$$

$$+\frac{\Delta_\theta}{\rho^2}\sin^2\theta\left(adt - \frac{r^2+a^2}{\Sigma}d\phi\right)^2, \tag{54}$$

where

$$\Delta_r = (r^2 + a^2)\left(1 + \frac{r^2}{\ell^2}\right) - 2Mr$$

$$\Sigma = 1 - \frac{a^2}{\ell^2},$$

$$\Delta_\theta = 1 - \frac{a^2}{r^2}\cos^2\theta,$$

$$\rho^2 = r^2 + a^2\cos^2\theta \tag{55}$$

ℓ is called as cosmological constant and Λ is cosmological constant where $\ell = \sqrt{-3/\Lambda}$, $\frac{M}{\Sigma}$ is the physical mass [9] $\frac{Ma}{\Sigma}$ is the angular momentum of Kerr Ads black hole [9]

7.1 Extremal limit

The black hole mass must satisfy the extremality condition [10]:

$$M \geq M_c = \frac{\ell}{3\sqrt{6}}\left[2\left(1 + \frac{a^2}{\ell^2}\right) + \sqrt{\left(1 + \frac{a^2}{\ell^2}\right)^2 + \frac{12a^2}{\ell^2}}\right] \tag{56}$$

$$\times\sqrt{\sqrt{\left(1 + \frac{a^2}{\ell^2}\right)^2 + \frac{12a^2}{\ell^2}} - \left(1 + \frac{a^2}{\ell^2}\right)}. \tag{57}$$

when $M = M_c$, the black hole is extremal. The angular velocity of the event horizon is given by

$$\Omega_H = \frac{a}{r_+^2 + a^2}\left(1 - \frac{a^2}{\ell^2}\right). \tag{58}$$

7.2 Wave equation for scalar perturbations

We study scalar perturbations in the Kerr-AdS background, considering a minimally coupled massless Klein-Gordon field. Using the Kerr-AdS metric from , the wave equation takes the explicit form [10]:

$$\frac{1}{\sqrt{-g}}\left(\sqrt{-g}\, g^{\mu\nu}\Phi_{,\mu}\right)_\nu = 0, \tag{59}$$

which expands to:

$$\left[\frac{\partial}{\partial r}\Delta_r\frac{\partial}{\partial r} + \frac{1}{\sin^2\theta}\frac{\partial}{\partial\theta}\Delta_\theta\sin\theta\frac{\partial}{\partial\theta} - \frac{1}{\Delta_r}\left((r^2+a^2)\frac{\partial}{\partial t} - a\Sigma\frac{\partial}{\partial\phi}\right)^2 + \frac{1}{\Delta_\theta}\left(a\sin\theta\frac{\partial}{\partial t} - \frac{\Sigma}{\sin\theta}\frac{\partial}{\partial\phi}\right)^2\right]\Phi = 0. \tag{60}$$

We decompose the wave function Φ using the separation of variable [7]:

$$\Phi(t,r,\theta,\phi) = e^{-i\omega t}e^{im\phi}R(r)S(\theta),$$

where:

- ω is a complex frequency
- m is an integer azimuthal quantum number

For waves co-rotating with the black hole ($m > 0$ when $\mathrm{Re}(\omega) > 0$), stability requires $\mathrm{Im}(\omega) < 0$. This decomposition yields two coupled ordinary differential equations:

Radial equation:

$$\left[\frac{d}{dr}\Delta_r\frac{d}{dr} + \frac{K_r^2}{\Delta_r} - \lambda\right]R(r) = 0, \tag{61}$$

Angular equation:

$$\left[\frac{d}{d\mu}\Delta_\mu\frac{d}{d\mu} - \frac{K_\mu^2}{\Delta_\mu} + \lambda\right]S(\mu) = 0 \tag{62}$$

with the following definitions:

$$K_r = -am\left(1 - \frac{a^2}{\ell^2}\right) + \omega(r^2 + a^2) \tag{63}$$

$$K_\mu = -\left(1 - \frac{a^2}{\ell^2}\right)am + \omega(a^2 - \mu^2) \tag{64}$$

$$\Delta_\mu = \left(1 - \frac{\mu^2}{\ell^2}\right)(a^2 - \mu^2), \mu = a\cos\theta. \tag{65}$$

7.3 Radial part

To solve radial differential equation we use Wronskian method ,we take same transformation like Teukolsky [7]

$$Y = (r^2 + a^2)^{1/2}R \tag{66}$$

$$\frac{dr_*}{dr} = \frac{r^2 + a^2}{\Delta_r}, \tag{67}$$

Then we get

$$\frac{d^2Y}{dr_*^2}+\left[\frac{K_r^2-\Delta_r\lambda}{(r^2+a^2)^2}-G^2-\frac{dG}{dr_*}\right]Y=0, \tag{68}$$

where

$$G=\frac{r\Delta_r}{(r^2+a^2)^2}. \tag{69}$$

when $r\to r_+$, $\Delta_r\to 0$ .It means near the event horizon eq becomes

$$\frac{d^2Y}{dr_*^2}+k^2Y\simeq 0, \quad \text{and} \quad k=\omega-\frac{am\Sigma}{r_+^2+a^2}, \tag{70}$$

then Y acts like

$$Y\sim e^{\pm ikr_*} \quad \text{as} \quad r_*\to-\infty(r\to r_+)$$

. As we know minus sign represents ingoing wave and plus sign represents outgoing wave and near the event horizon wave function should be negative so wave function should be like

$$Y\sim e^{-ikr_*} \quad \text{as} \quad r_*\to-\infty(r\to r_+)$$

Now ,for the large $r(r\to\infty)$, eq looks like

$$(r^2+1)\frac{d}{dr}\left((r^2+1)\frac{dY}{dr}\right)+\left\{\omega^2-\frac{\lambda}{\ell^2}-\frac{a^2}{\ell^2}\left(1+\frac{r^2}{\ell^2}\right)-\frac{2ir\omega}{\ell^2}+O\left(\frac{1}{r}\right)\right\}Y=0, \tag{71}$$

As r_* approaches a finite value, this indicates that infinity acts as a regular singular point for Eq. (68). Consequently, the solution Y behaves asymptotically as:

$$Y\sim Ar^{-2}+Br \quad \text{as} \quad r\to\infty, \tag{72}$$

where A and B are constants. To ensure physical consistency, we must enforce the boundary

condition $Y\to 0$ as $r\to\infty$; otherwise, Y would diverge at infinity. For numerical integration, we employ the Runge-Kutta method to solve Eq. (68). The integration is performed in two stages:

1. **Outward integration** starting from near the horizon $r\approx r_+$.

2. **Inward integration** from a large radius $R \approx 100 r_+$.

These solutions are then matched at an intermediate point $r = r_m$ (where $r_+ < r_m < R$). To initialize the integration, we express the solutions as power series expansions around the horizon and infinity. Near the horizon, the solution takes the form of a power series:

Near the event horizon ($r \approx r_+$), the solution takes the form of a power series expansion:

$$Y = e^{-ikr_*} \left[b_0 + b_1(r - r_+) + b_2(r - r_+)^2 + b_3(r - r_+)^3 + \cdots \right], \tag{73}$$

where k is a wave number parameter.

For large distances ($r \to \infty$), the solution behaves as:

$$Y = \frac{1}{r^2} \left(c_0 + \frac{c_1}{r} + \frac{c_2}{r^2} + \frac{c_3}{r^3} + \cdots \right). \tag{74}$$

The coefficients b_n (for $n = 1, 2, 3, \ldots$) are recursively determined from the leading coefficient b_0.

Similarly, the coefficients c_n are derived from c_0.

While we omit explicit expressions here, these coefficients can be systematically calculated through straightforward derivation.

We construct two numerical solutions:

Y_1: Integrated outward from near the horizon ($r \approx r_+$)

Y_2: Integrated inward from a large radius ($r = R$)

These solutions are matched at an intermediate point $r = r_m$. Their compatibility is tested using the Wronskian:

$$W(Y_1, Y_2) = Y_1 \frac{dY_2}{dr_*} - Y_2 \frac{dY_1}{dr_*} = F(\omega, \lambda). \tag{75}$$

7.4 2. Angular Part: Solving the Spheroidal Harmonic Equation

7.4.1 Boundary Conditions and Series Solution

To determine the angular separation constant λ, we employ the continued fraction method . The angular equation (62) contains regular singular points at $\mu = \pm a$, requiring solutions $S(\mu)$ to remain finite at both boundaries. This leads to the asymptotic behavior [10]:

$$S(\mu) \to \begin{cases} (\mu + a)^{|m|/2} & \text{as } \mu \to -a, \\ (\mu - a)^{|m|/2} & \text{as } \mu \to a \end{cases} \tag{76}$$

A general solution satisfying these conditions can be expressed as a series expansion [10]:

$$S(\mu) = (a-\mu)^{m/2}(a+\mu)^{m/2}(\ell-\mu)^{-((\omega\ell/2)+(am/2\ell))} \quad \times (\ell+\mu)^{((\omega\ell/2)+(am/2\ell))} \sum_{n=0}^{\infty} a_n \frac{(a+\mu)^n}{(2a)^n}. \tag{77}$$

7.4.2 Recurrence Relations

Substituting all this solution we get recurrence relations for the coefficients a_n:

$$\alpha_0 a_1 + \beta_0 a_0 = 0 \tag{78}$$

$$\alpha_1 a_2 + \beta_1 a_1 + \gamma_1 a_0 = 0 \tag{79}$$

$$\alpha_n a_{n+1} + \beta_n a_n + \gamma_n a_{n-1} + \delta_n a_{n-2} = 0 \quad (n \geq 2), \tag{80}$$

where the coefficients $\alpha_n, \beta_n, \gamma_n, \delta_n$ are given by:

$$\alpha_n = (n+1)\left(1 - \frac{a^2}{\ell^2}\right)(n+m+1) \tag{81}$$

$$\beta_n = -\left(1 - \frac{5a^2}{\ell^2}\right)n^2 + \left(\frac{5a^2}{\ell^2} + \frac{10a^2 m}{\ell^2} - 2m - 1 + 4a\omega\right)n \tag{82}$$

$$-m^2 - m + 4am\omega + 2a\omega + \lambda + \frac{5a^2 m}{\ell^2}(m+1) \tag{83}$$

$$\gamma_n = 4\left\{-\frac{2a^2 n^2}{\ell^2} - \left(a\omega + \frac{4a^2 m}{\ell^2}\right)n - am\omega + \frac{2a^2}{\ell^2}(1-m^2)\right\}, \tag{84}$$

$$\delta_n = 4\frac{a^2}{\ell^2}\left\{n^2 + n(2m-1) - 2 + m^2 - m\right\}. \tag{85}$$

7.4.3 Gaussian Reduction to Three-Term Recurrence

Since the continued fraction method requires a three-term recurrence relation, we perform Gaussian reduction on the four-term system (80). The transformed coefficients become:

$$\alpha'_n = \alpha_n \tag{86}$$

$$\beta'_n = \beta_n \tag{87}$$

$$\gamma'_n = \gamma_n \quad \text{for } n = 0, 1 \tag{88}$$

$$\alpha'_n = \alpha_n \tag{89}$$

$$\beta'_n = \beta_n - \frac{\alpha'_{n-1}}{\gamma'_{n-1}}\delta_n \tag{90}$$

$$\gamma'_n = \gamma_n - \frac{\beta'_{n-1}}{\gamma'_{n-1}}\delta_n \quad \text{for } n \geq 2. \tag{91}$$

7.4.4 Convergence Criterion and Quantization Condition

The boundary condition at $\mu = a$ is satisfied if and only if the series $\sum_{n=0}^{\infty} a_n$ converges. This translates to a continued fraction equation:

$$0 = \beta'_0 - \cfrac{\alpha'_0\gamma'_1}{\beta'_1 - \cfrac{\alpha'_1\gamma'_2}{\beta'_2 - \cdots}} \equiv G(\omega, \lambda), \tag{92}$$

which implicitly defines a quantization condition for λ as a function of ω. Numerical root-finding of $G(\omega, \lambda) = 0$ yields the allowed eigenvalues λ for quasinormal modes.

7.5 Result

After using Wronskian method for radial part and continued fraction method for angular part , we get two equation like G(ω,λ)=0 and F(ω,λ)=0 and get result of quasi normal mode of Kerr Ads black hole at extremal limit .

For $l = 1, m = 1$

Rotation Parameter (a)	λ		omega	
	Real	**Imaginary**	**Real**	**Imaginary**
0.2000	5.841296	-0.134143	0.739999	-0.175674
0.2250	5.812394	-0.137345	0.740000	-0.182107
0.2500	5.766081	-0.136704	0.740000	-0.183603
0.2750	5.766081	-0.136704	0.825556	-0.210820
0.3000	5.689980	-0.136916	0.825553	-0.215717
0.3500	5.496444	-0.139939	0.825550	-0.234218
0.4000	5.496444	-0.139939	1.395133	-0.680146
0.4200	5.333657	-0.125686	1.395104	-0.690734
0.4900	4.240491	-0.072771	1.395106	-0.715445

For $l = 1, m = 0$

Rotation Parameter (a)	λ		omega	
	Real	**Imaginary**	**Real**	**Imaginary**
0.2000	1.602845	-0.132396	0.739995	-0.176676
0.2250	1.650931	-0.156470	0.739995	-0.191038
0.2500	1.694074	-0.170871	0.739995	-0.192512
0.2750	1.694074	-0.170871	0.700060	-0.176803
0.3000	1.726741	-0.189357	0.700060	-0.183281
0.3500	1.781666	-0.236669	0.700059	-0.203368
0.4000	1.781666	-0.236669	0.670230	-0.181583
0.4200	1.792584	-0.255482	0.670202	-0.188708
0.4900	1.800568	-0.307584	0.670201	-0.201698

For $l = 1, m = -1$

Rotation Parameter (a)	λ		omega	
	Real	**Imaginary**	**Real**	**Imaginary**
0.2000	-0.045333	-0.208290	0.740000	-0.173575
0.2250	0.083375	-0.247428	0.740000	-0.183280
0.2500	0.214167	-0.276287	0.740000	-0.184192
0.2750	0.214167	-0.276287	0.659470	-0.167447
0.3500	0.589053	-0.457712	0.659470	-0.217958
0.4000	0.589053	-0.457712	0.550994	-0.190713
0.4200	0.682471	-0.501004	0.550981	-0.198811

7.5.1 Plotting comparison between $r_+ = 1.0$'s data and extremal limit's data

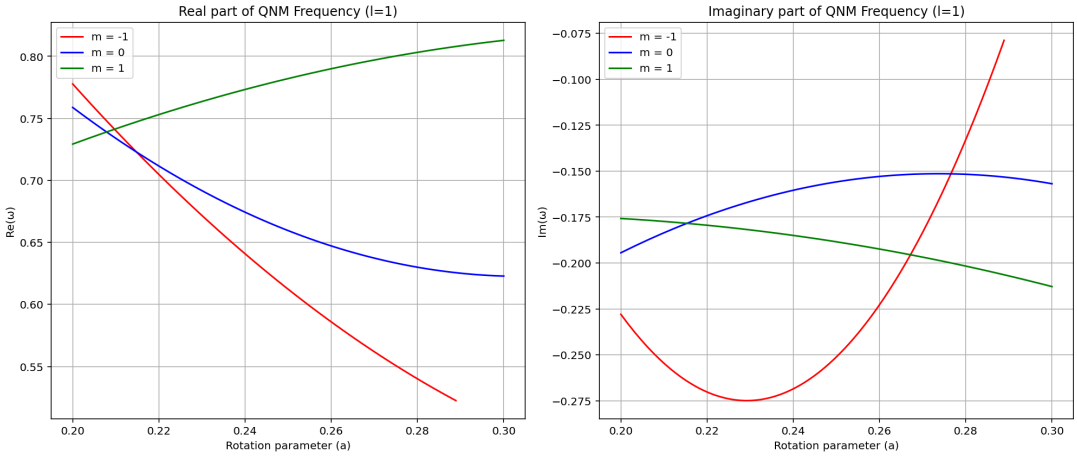

Figure 4: quasi normal frequencies vs rotation parameter(a) for extremal limit

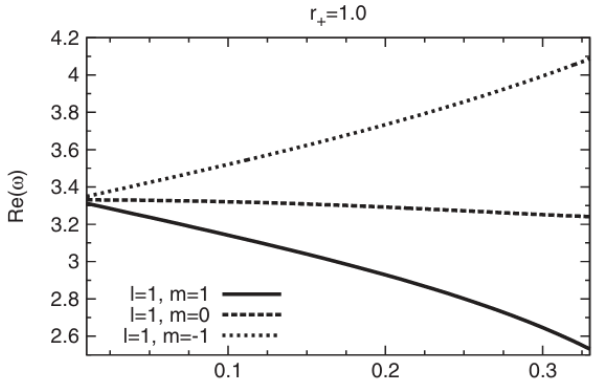

Figure 5: realω vs rotation parameter(a) for $r_+ = 1.0$

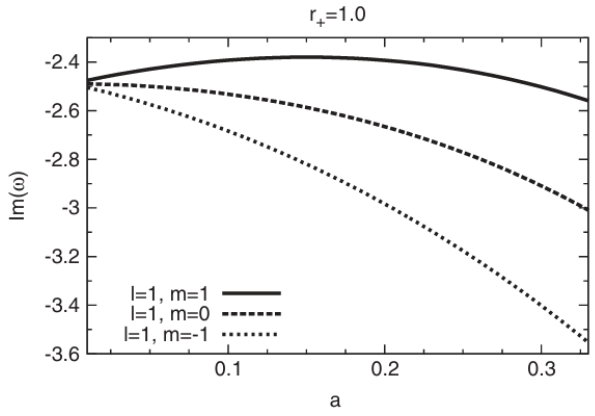

Figure 6: imaginaryω vs rotation parameter(a) for $r_+ = 1.0$

8 Conclusion

In this study, we explore the quasi-normal modes (QNs) of an extremal Kerr Ads black hole for the specific case of angular quantum number $l = 1$. Our investigation focuses on how the QN frequencies ω behave as we vary the rotation parameter a, revealing intriguing patterns in both their real ($\mathrm{Re}\,\omega$) and imaginary ($\mathrm{Im}\,\omega$) components that depend critically on the azimuthal quantum number m:

- For $m = +1$, we observe that as a increases, $\mathrm{Re}\,\omega$ grows while $\mathrm{Im}\,\omega$ becomes less negative.
- For $m = 0$, both $\mathrm{Re}\,\omega$ and $\mathrm{Im}\,\omega$ decrease monotonically with increasing a.
- The $m = -1$ case shows behavior similar to $m = 0$, with both real and imaginary parts decreasing as a increases.

A key result from our numerical analysis is that $\mathrm{Im}\,\omega < 0$ holds universally across all modes studied. This negative imaginary component guarantees that perturbations will decay exponentially over time rather than grow. The absence of any unstable modes (where $\mathrm{Im}\,\omega > 0$) in our spectrum provides compelling support for the *linear stability* of extremal Kerr-AdS black holes within the framework of Einstein gravity.

References

[1] Nuclear Physics B - Proceedings Supplements Volume 216, Issue 1, July 2011, Pages 194-210

[2] Compère, G. The Kerr/CFT correspondence and its extensions. Living Rev Relativ 20, 1 (2017)

[3] Dennis Hansen, Niels Bohr Institute University of Copenhagen, Killing-Yano tensors. August 13, 2014

[4] James Bardeen and Gary T. Horowitz Phys. Rev. D 60, 104030 – Published 26 October 1999

[5] Leaver, Proc. R. Soc. A 402, 285 (1985)

[6] Baber, W.G., Hasse, H.R. 1935 ´ Proc. Cambridge Phil. Soc. 25, 564

[7] Teukolsky, S.A. 1972 Phys. Rev. Lett. 29, 1114

[8] B. Carter, Commun. Math. Phys. 10, 280 (1968).

[9] G.W. Gibbons, M.J. Perry, and C.N. Pope, Classical Quantum Gravity 22, 1503 (2005).

[10] Nami Uchikata*, Shijun Yoshida†, and Toshifumi Futamase‡,Phys. Rev. D 80, 084020 (2009)